European Journal of Pharmaceutics and Biopharmaceutics 77 (2011) 122–131

Contents lists available at ScienceDirect

European Journal of Pharmaceutics and Biopharmaceutics

journal homepage: www.elsevier.com/locate/ejpb

Research paper

Solid dispersions in the development of a nimodipine floating tablet formulation and optimization by artificial neural networks and genetic programming

Panagiotis Barmpalexis, Kyriakos Kachrimanis *, Emanouil Georgarakis

Department of Pharmaceutical Technology, Aristotle University of Thessaloniki, Thessaloniki, Greece

ARTICLE INFO

Article history:
Received 31 May 2010
Accepted in revised form 30 September 2010
Available online 8 October 2010

Keywords:
Solid dispersions
Nimodipine
Controlled release
Effervescent floating tablets
Artificial neural networks
Genetic programming

ABSTRACT

The present study investigates the use of nimodipine–polyethylene glycol solid dispersions for the development of effervescent controlled release floating tablet formulations. The physical state of the dispersed nimodipine in the polymer matrix was characterized by differential scanning calorimetry, powder X-ray diffraction, FT-IR spectroscopy and polarized light microscopy, and the mixture proportions of polyethylene glycol (PEG), polyvinyl-pyrrolidone (PVP), hydroxypropylmethylcellulose (HPMC), effervescent agents (EFF) and nimodipine were optimized in relation to drug release (% release at 60 min, and time at which the 90% of the drug was dissolved) and floating properties (tablet's floating strength and duration), employing a 25-run D-optimal mixture design combined with artificial neural networks (ANNs) and genetic programming (GP). It was found that nimodipine exists as mod I microcrystals in the solid dispersions and is stable for at least a three-month period. The tablets showed good floating properties and controlled release profiles, with drug release proceeding via the concomitant operation of swelling and erosion of the polymer matrix. ANNs and GP both proved to be efficient tools in the optimization of the tablet formulation, and the global optimum formulation suggested by the GP equations consisted of PEG = 9%, PVP = 30%, HPMC = 36%, EFF = 11%, nimodipine = 14%.

1. Introduction

Nimodipine belongs to the class of pharmacological agents known as calcium channel blockers. It exists into two polymorphs known as mod I and II. Mod I is the racemic crystal (containing an equimolar ratio of the two enantiomers in the lattice) while mod II is the conglomerate (equimolar mixture of pure R and S enantiomer crystals) [1]. Oral administration of nimodipine is associated with certain problems such as frequent dosing (30–60 mg every 4–8 h), varying half-life and fluctuating plasma concentrations [2], problems that can possibly be addressed by the preparation of a controlled release formulation [3–5]. Floating tablet formulations could be an appealing solution, as they can prolong the residence time of the dosage form in the stomach and thus extend the release of the active pharmaceutical ingredients (APIs) [6–8]. These formulations usually consist of swellable polymers, such as methylcellulose or chitosan, and various effervescent compounds, such as sodium bicarbonate, tartaric acid and citric acid [9]. One of the main drawbacks of effervescent floating formulation is the extent of initial burst effect due to excess CO_2 generation. Reducing the proportion of effervescent compounds could solve the problem; however, this usually leads to limitations in floating ability.

An alternative way to restrain burst effect is by the use of solid dispersions as drug carriers, a technique that is proven to be efficient [10] without the need to reduce the proportion of the effervescent agents in the formulation. The term "solid dispersions" refers to a family of multi-component systems whereby a crystalline or amorphous drug is dispersed into an amorphous or semi-crystalline polymer matrix [11]. The release rate of the resultant formulations is greatly affected by the physical state of the dispersed drug, which in turn is defined by the solubility of the drug in the polymer, the method of preparation, the use of plasticizing excipients, etc. Therefore, the development of a floating controlled release formulation based on a solid dispersion drug carrier system involves handling and optimizing a large number of variables. According to the recent FDA initiative in the industry [12,13], as well as the ICH Q8 Pharmaceutical Development guidance [14], pharmaceutical development problems of this kind are nowadays addressed in terms of the newly introduced concepts of quality by design (QbD), process analytical technologies (PAT) and design of experiments (DOE). This approach requires the application of systematic optimization techniques based on experimental design, combined with the use of novel, highly efficient model-fitting

* Corresponding author. Department of Pharmaceutical Technology, School of Pharmacy, Aristotle University of Thessaloniki, 54124 Thessaloniki, Greece. Tel.: +30 2310997666; fax: +30 2310997652.
E-mail address: kgk@pharm.auth.gr (K. Kachrimanis).

0939-6411/$ - see front matter © 2010 Elsevier B.V. All rights reserved.
doi:10.1016/j.ejpb.2010.09.017

methods, such as machine learning algorithms (artificial neural networks (ANN) and genetic programming, (GP)) [5,15,16].

Therefore, the present study investigates the use of solid dispersions in the development of a nimodipine effervescent floating formulation. The physical state of nimodipine in the dispersions is characterized by optical microscopy, thermal analysis, powder X-ray diffraction and FT-IR spectroscopy. The mechanism of drug release from the polymer matrices is evaluated on the basis of swelling and erosion studies, while controlled release and floating ability are achieved by optimizing the composition of the solid dispersions according to a statistical experimental design combined by novel machine learning algorithms, such as GP [17] and ANNs [5,18,19].

2. Materials and methods

2.1. Materials

Micronized nimodipine powder (mean circle equivalent diameter of 18.2 ± 11.2 μm, [5]), supplied by Union Farmaceutics S.A. (UQUIFA) (Barcelona, Spain), was used as an active pharmaceutical ingredient (API).

Polyethylene glycol (PEG 4000, CLARIANT, Sulzbach, Germany) was used as polymeric carrier for the dispersion of NIM. Hydroxypropylmethylcellulose (HPMC K100, Dow Chemical Company, Midland, MI, USA) was used as swelling agent, while sodium bicarbonate and citric acid (Sigma Chemicals Co., St. Louis, MO, USA) were used as effervescent agents (EFF) to induce tablet floatation. Polyvinylpyrrolidone (PVP K30, BASF Co., Ledgewood, NJ, USA) was added to the dispersions in order to increase gel cohesion during dissolution.

Magnesium stearate (Mg Stearate, Katayama, Osaka, Japan) at a 0.5% w/w ratio was used as a lubricant for tableting, while 0.5% w/w sodium lauryl sulfate (SLS, COGNIS, Fino Mornasco, Italy) was added to the dissolution medium to ensure sink conditions. All other materials and reagents were of analytical grade and used as received.

2.2. Preparation of solid dispersions and tableting

Pre-weighted amounts of PEG (melting point at 61.2 °C) were placed in aluminium dishes and heated in a water bath at 70 °C to complete melting. Nimodipne was dispersed in the melt and stirred for 5 min. The remaining constituents (polymers and gas-generating agents, sodium bicarbonate and citric acid in 1:1 w/w ratio) were added sequentially at 5 min intervals. The resultant dispersions were stored at −18 °C for 5 days and then pulverised manually using a mortar and a pestle. The 100–150 mesh size fraction was separated by sieving, and Mg Stearate (0.5% w/w) was added and mixed for 5 min with a spatula. The dispersions were stored in hermetically sealed dark-glass jars for further processing.

Appropriate amounts of sample containing 30 mg of nimodipine were compressed on a manually operated hydraulic press equipped with a 10 mm diameter flat-faced punch and die set, pre-lubricated with Mg Stearate, at a compression pressure of 1561 Nt/cm^2 applied for 5 s (sufficient to obtain compacts of minimum attainable porosity).

2.3. Physical characterization of solid dispersions

2.3.1. Optical polarized light and hot-stage microscopy

Polarized light microscopy was applied according to the European Pharmacopoeia method for the detection of crystallinity [20]. Microscopic observations of the crystalline samples were performed on an Olympus BX41 polarized light microscope (Olympus, Japan) to observe the birefringence in the examined samples.

2.3.2. Powder X-ray diffraction (PXRD)

PXRD patterns of the raw materials, their physical mixtures and the prepared solid dispersions were measured on a Rigaku Miniflex II powder diffractometer with a nickel-filtered radiation. The patterns were recorded on a quartz plate at a tube voltage of 30 kV and a current of 15 mA applying a scan rate of 0.05° 2θ/s in the angular range of 5–45° 2θ. The peak intensities and 2θ values of the solid dispersion patterns were compared to those of the pure materials in order to evaluate the physical form of nimodipine in the samples.

2.3.3. Fourier-transform infrared spectroscopy (FT-IR)

FT-IR spectra in the region of 500–3500 cm^{-1} for both starting materials and solid dispersions were obtained using a Shimadzu IR-Prestige-21 FT-IR spectrometer coupled with a horizontal Golden Gate MKII single-reflection ATR system (Specac, Kent, UK) equipped with a ZnSe lense, after appropriate background subtraction. Thirty-two scans over the selected wave number range at a resolution of 4 cm^{-1} were averaged for each sample.

2.3.4. Differential scanning calorimetry (DSC)

DSC determinations were carried out on a Shimadzu DSC-50 thermal analyzer (Shimadzu Corporation, Japan). Accurately weighted amounts of samples (3–5 mg) were placed in perforated aluminium pans and scanned through a temperature range of 20–140 °C at a heating rate of 10 °C/min, under a nitrogen purge gas flow of 25 mL/min. The instrument was calibrated for temperature and energy using indium standards.

In order to estimate the long-term storage stability of the solid dispersions, all determinations were repeated after storage for 3 months at two different temperatures and relative humidity (RH) conditions (25 °C – 60% RH, and 40 °C – 75% RH).

2.4. Dissolution studies

After verification of the drug content of the tablets, dissolution testing was performed by the rotating paddle USP apparatus II, (Distek 2100C, North Brunswick, NJ) at 37 °C ± 0.5 °C and 50 rpm, using 1000 ml of aqueous solution containing 0.5% (w/w) SLS. Sink conditions were maintained throughout the test. Four milliliter aliquots were collected at 5, 15, 30, 60, 120, 240, 480, 720, 960 and 1200 min using an automatic sampler (Distek Evolution 4300) and assayed immediately for nimodipine content.

All determinations were performed in triplicate following a validated HPLC method [21] on a Prominence HPLC system (Shimadzu Corporation, Japan) consisting of a degasser (Model DGU-20A5), a pump (Model LC-20AD), an auto sampler (Model SIL-20AC), a UV–Vis detector (Model SPD-20A) and a column oven (Model CTO-20AC). Chromatographic analysis was performed on an Interchrom C_8 analytical column (5 μm particle size, 250 × 4.6 mm I.D.). The mobile phase used was acetonitrile/water (67.5:32.5, v/v), and the analytes were detected at 236 nm. The flow rate of the mobile phase was 0.9 ml/min, and the column temperature was 40 °C. Injection volume was set at 10 μl. The excipients used in this study did not interfere with the chromatographic analysis of Nimodipine.

2.5. Floating behavior of tablets

The in vitro floating behavior of the tablets in the selected dissolution medium (1000 ml) was evaluated in terms of floating duration (FLD) and strength (Fs). Floating duration of the tablets was determined by visual observation during the dissolution study. The resultant weight of the tablet in immersed conditions was determined using an on line continuous monitoring apparatus proposed by Timmermans and Moës [22]. Briefly, in each experimental trial, a tablet was placed in the sample holder basket, hang-

ing from an analytical balance connected to a PC. The holder was immersed at a fixed depth into the dissolution vessel, and data were logged every 5 min for up to 1200 min. The vessel was covered in order to prevent water evaporation. After a certain lag time, the tablet started to float and the floating strength of the tablet was determined by measuring the weight diminution.

2.6. Swelling and erosion studies

Matrix swelling, described as water absorption capacity, was determined gravimetrically on a modified USP apparatus consisting of a 200-mesh stainless steel basket carrying the tablet, mounted above the stirring paddle rotating at 50 rpm [23,24]. Baskets containing the tablets were immersed in 1000 ml of dissolution medium at 37 °C ± 0.5 °C, and periodically detached from the apparatus, blotted with absorbent tissue to remove any excess dissolution medium on the surface and weighed. Degree of swelling (% water uptake) was calculated according to the following equation:

$$\text{Degree of swelling } (\%\text{ water uptake}) = \left[\frac{W_t - W_o}{W_o}\right] \times 100 \qquad (1)$$

where W_o is the initial weight of the dry tablet, and W_t is the weight of the wet, swollen tablet.

Matrix erosion was determined at the same time intervals, on the same tablets used for the swelling determinations. After weighing, the hydrated matrices were dried in an oven at 50 °C for 24 h and the remaining dry weight, W_r, was determined. Matrix erosion was calculated according to the formula:

$$\text{Erosion } (\%\text{ mass loss}) = \left[\frac{W_o - W_r}{W_o}\right] \times 100 \qquad (2)$$

The mass loss due to the dissolution of nimodipine was considered negligible.

The values of dissolution medium uptake per unit mass of matrix remaining were fitted to a square root equation for the initial points, where a linear relationship existed between uptake and square root of time [25]:

$$\left[\frac{W_t - W_o}{W_o}\right] \times 100 = a \times t^{0.5} \qquad (3)$$

where a is the dissolution medium uptake rate constant and t is the time. The values of the dry weight data were fitted to a modification of the cube root relationship (Hixson–Crowell model) reported by Tahara et al. [26], in order to determine the apparent polymer erosion rate constant k_2:

$$\left[\frac{W_o - W_r}{W_o}\right]^{1/3} = 1 - k_2 t \qquad (4)$$

2.7. Optimization of flotation and drug release

In order to achieve a desirable flotation and release profile, the effects of five formulation factors, namely the proportion of PEG (X_1), PVP (X_2), HPMC (X_3), effervescent agents (sodium bicarbonate and citric acid 1:1 w/w (X_4)), and nimodipine (X_5), were evaluated on four response variables: two variables characterizing the floating ability of the tested formulation (measured floating strength, Fs, and duration, FLD), and two describing the release profile (percent of drug dissolved at 60 min, $Y_{60\text{min}}$, which is indicative of the existence of an initial burst effect, and the time at which the 90% of the drug was dissolved, $t_{90\%}$, which is indicative of release prolongation).

Factor levels were optimized following a D-optimal mixture experimental design (Table 1), which is a special case of fractional factorial design that allows great flexibility especially in cases where the area of interest (experimental domain) is reduced to an irregular polyhedron [27]. ANN and GP were used as model-fitting tools instead of the conventional MLR equations.

Table 1
Experimental domain according to the D-optimal mixture design applied in this study.

Code	Independent variables examined (%)				
	PEG (X_1)	PVP (X_2)	HPMC (X_3)	EFF*(X_4)	NIM+ (X_5)
F1	9.00	30.00	40.00	16.00	5.00
F2	9.00	25.00	40.00	12.00	14.00
F3	9.50	30.00	30.50	16.00	14.00
F4	13.00	30.00	40.00	8.00	9.00
F5	13.75	27.50	35.25	14.00	9.50
F6	14.00	25.00	40.00	16.00	5.00
F7	14.50	20.00	40.00	16.00	9.50
F8	14.50	20.00	40.00	16.00	9.50
F9	15.00	25.00	30.00	16.00	14.00
F10	18.00	30.00	30.00	8.00	14.00
F11	18.00	30.00	30.00	8.00	14.00
F12	18.00	20.00	40.00	8.00	14.00
F13	19.00	30.00	30.00	16.00	5.00
F14	20.75	25.00	35.00	12.00	7.25
F15	22.00	30.00	35.00	8.00	5.00
F16	22.00	25.00	40.00	8.00	5.00
F17	23.00	20.00	35.00	8.00	14.00
F18	24.00	20.00	30.00	12.00	14.00
F19	24.00	20.00	30.00	12.00	14.00
F20	27.00	30.00	30.00	8.00	5.00
F21	27.00	20.00	40.00	8.00	5.00
F22	28.00	20.00	31.00	16.00	5.00
F23	28.00	20.00	31.00	16.00	5.00
F24	28.00	24.50	30.00	8.00	9.50
F25	28.00	24.50	30.00	8.00	9.50

* *EFF = effervescent agents, sodium bicarbonate and citric acid (1:1 w/w).*
\+ *NIM = Nimodipine.*

2.7.1. Artificial neural network

A feed-forward back-propagation network consisting of five inputs (each corresponding to a formulation factor) and four output units (each corresponding to a selected response) was fitted to the data collected according to the D-optimal design. Twenty-one formulations were randomly selected from the D-optimal mixture design and assigned to the training set while the remaining were used as a validation set. The logistic sigmoid function was used as activation function for all units, and the input and output patterns were scaled from 0 to 1. The 'vanilla' or standard back-propagation (StBack) training algorithm was selected, and the 'early stopping' method was applied in order to avoid network's overtraining. Causal and predictive importance of the input variables (sensitivity and saliency, respectively) was calculated according to Kachrimanis et al. [28], as described in Ref. [5]. Specifically, sensitivity is defined as the change of the output corresponding to a given change in an input variable, while saliency refers to the increase in the error function when an input is omitted from the network. Subsequently, pruning (size reduction by removal of unnecessary units and/or links) by the magnitude-based pruning (MBP) algorithm was performed in order to simplify the network. The Stuttgart Neural Network Simulator (SNNS version 4.2 for WIN32) software package was employed for the development, training and size reduction of the ANN.

2.7.2. Symbolic regression via GP

GP is a systematic method for getting the computers to automatically solve a problem [29]. Based on Darwin's Natural Selection theory that individuals who better adapt to the environment have a greater chance of surviving and passing their genetic char-

Table 2
Control parameters and their ranges used in GP.

Population size	500–1000–2000
Generations	100–150–200
Crossover rate	0.3–0.4–0.5
Mutation rate	0.3–0.4–0.5
Fitness function	SSE
Function set	+, ∗, /, -, ^, cos, sin, tan, exp, log
Constant range	−10 to 10 by 0.001
Constant probability	0.2–0.5
Elitism	1
Tournament size	3–7

acteristics to their offspring, GP automatically generates programs in order to 'naturally' select the one that better solves an investigated problem [30]. When the generated programs represent mathematical equations, the process of finding the best-fitting equation with the aid of GP is called symbolic regression [29]. The GP evolutionary process starts with the generation of a random initial population, and the algorithm enters a loop that is executed until a desired solution is found. The loop consists of two major tasks: (1) evaluate each program (equation) by comparing each solution to the ideal one (this is made through a 'fitness' function) and (2) create a new population by applying basic genetic operations such as 'reproduction', 'crossover' and 'mutation' [30]. The efficiency of the process is determined by a set of parameters (such as crossover rate, mutation rate, population size, tournament size) that control the way in which the search for the ideal solution is conducted [29].

In the present study, the SyMod software package, freely available for download at http://www.s.org, was used for genetically developing nonlinear mathematical equations. The sum of squared error (SSE) was used as fitness function. The ranges of the parameters tested in genetic programming are summarized in Table 2.

Table 3
Experimental domain and measured responses for the external validation (test) set used for validating ANN and GP prediction performance.

Code	Independent variables (%)					Measured responses			
	X_1	X_2	X_3	X_4	X_5	Y_{60min}[a] (%)	$t_{90\%}$[b] (h)	FLD[c] (h)	Fs[d] (g)
FA	18	20	40	14	8	33.25	12.01	14.50	1.69
FB	14	24	40	8	14	28.45	13.45	14.07	0.44
FC	11	25	40	10	14	28.23	12.99	15.33	0.46
FD	10	26	40	10	14	29.00	13.87	14.70	0.40
FE	13	26	40	9	12	25.30	15.87	13.65	0.42

SD: a = 0.81–2.16, b = 0.09–0.63, c = 0.33–0.91, d = 0.02–0.58.

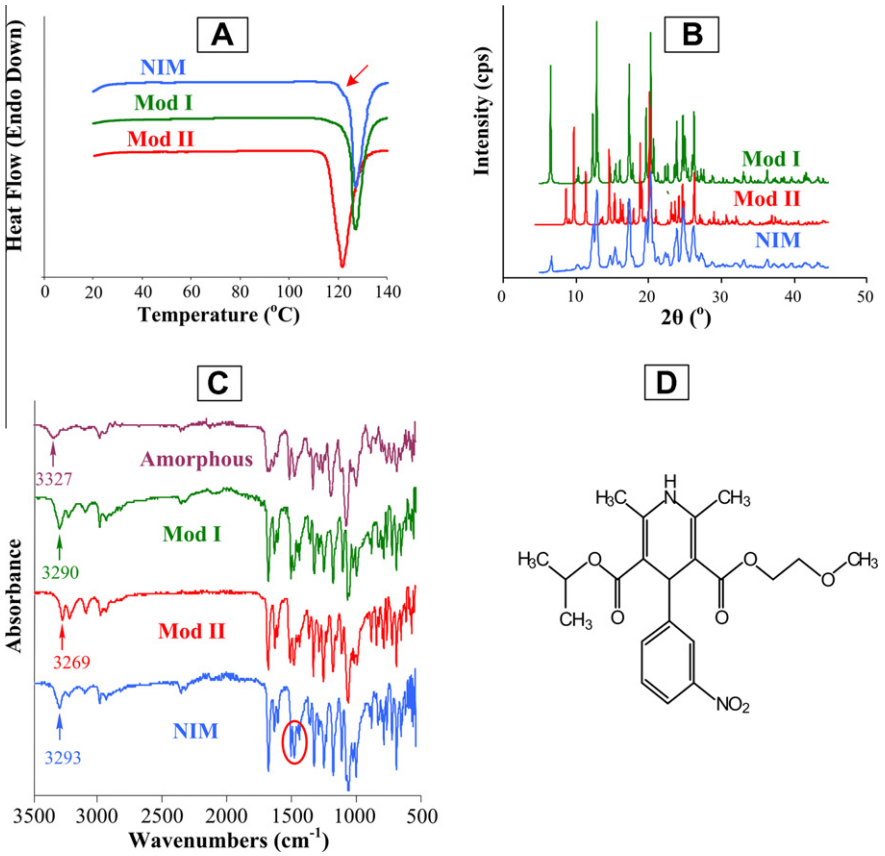

Fig. 1. DSC thermograms (A), PXRD diffractograms (B) and FT-IR spectra (C) of amorphous, crystalline mod I and II, and commercial nimodipine, together with the molecular structure representation (D).

2.8. Validation of ANN and GP, global optimization

The developed ANN and GP models were compared for prediction ability on the basis of Root Mean Squared Error of Prediction (RMSEp) using an external validation set consisting of five formulations having maximum proportion levels of HPMC (40%) in order to ensure that a gel layer strong enough to enclose the generated CO_2 and ensure floating conditions was achieved (Table 3). The remaining proportions were selected randomly.

In order to investigate the best model's ability to locate an actual global optimum solution, the minimization of the standardized Euclidian distance between the predicted value of each response and the desirable levels (maximum floating, floating duration over 9 h, minimum burst effect and 90% of the drug released in 12 h), Eq. (5), was selected as an appropriate global optimization tool [31].

$$S(X) = \left[\sum_{k}^{n}\left(\frac{O_k(X) - E_k(X)}{SD_k}\right)^2\right]^{1/2} \quad (5)$$

where $S(X)$ is the distance function generalized by the standard deviation (SD_k) of the observed values for each response (k), X is the set of independent variables examined, $O_k(X)$ and $E_k(X)$ are the optimum value and the estimated value of the response, k. A trial-and-error method was employed, starting from different initial conditions, in order to avoid local minima.

3. Results and discussion

3.1. Physical characterization of solid dispersions

Fig. 1A–D presents DSC thermograms, PXRD diffractograms and FT-IR spectra of the commercial nimodipine powder used as starting material in this study, and that of pure modifications I and II crystallized from ethanol solution, together with the molecular structure of NIM.

DSC thermograms, Fig. 1A, show that mod I and II crystals melt at 127.1 and 121.3 °C, respectively, in agreement with literature data [1]. The commercial nimodipine sample exhibits an endothermic peak at 127.1 °C, preceded by a shoulder that is probably associated with melting of mod II crystals, and indicates the presence of mod II in the raw material used in this study.

The PXRD patterns, Fig. 1B, show a high similarity between the two crystal modifications of nimodipine (mod I and II). Characteristic differences lie in the low 2θ reflections (6.7° 2θ for mod I, and 10.4° and 12.0° 2θ for mod II) that can be used for the identification of the two crystal forms. Based on the 6.7° 2θ reflection, the PXRD patterns of the commercial raw material correspond to mod I, however, a weak reflection at 12.0° 2θ indicates the presence of a small amount of mod II crystals, in agreement with the DSC observations.

FT-IR spectra of amorphous and crystalline nimodipine mod I and II, shown in Fig. 1C, indicate that the most characteristic difference between amorphous nimodipine and mods I and II lies in the

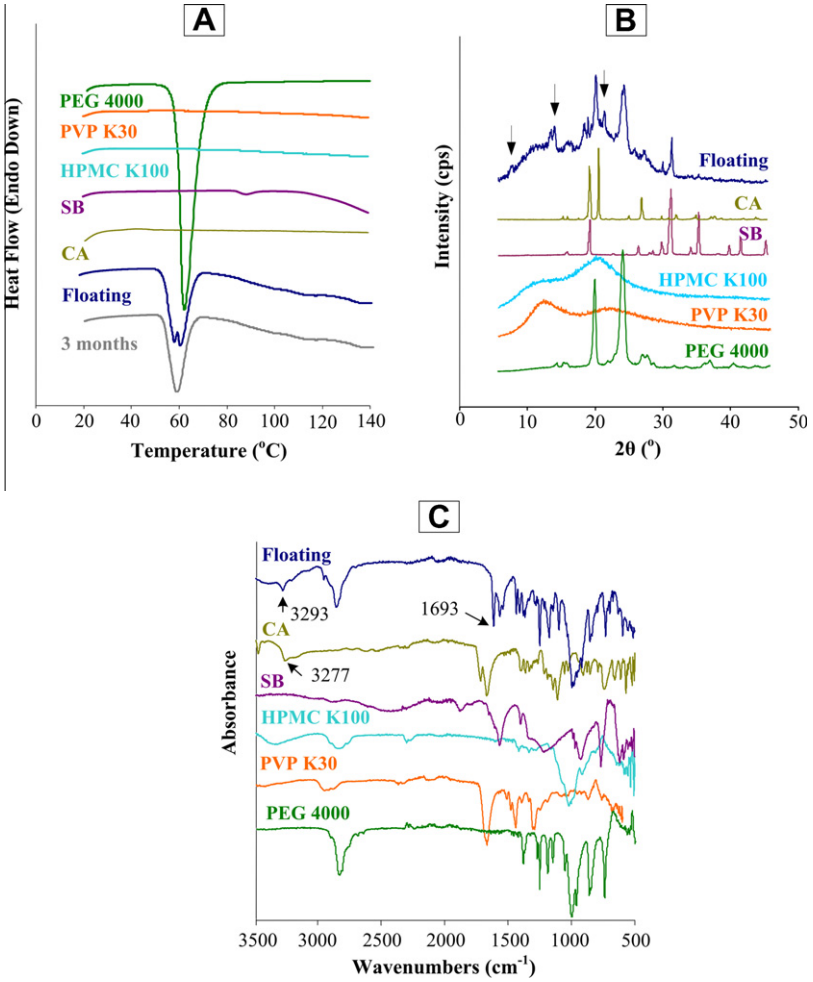

Fig. 2. DSC thermograms (A), PXRD diffractograms (B) and FT-IR spectra (C) of PEG 4000, PVP K30, HPMC K100, SB, CA, and a representative effervescent floating solid dispersion (formulation F15).

N–H stretch (3327 cm^{-1}, 3290 cm^{-1}, and 3269 cm^{-1}, respectively) and is due to hydrogen bonding between the NH group and the ether or carbonyl oxygen for the crystalline or amorphous material, respectively [32]. Further differences between the two polymorphs are observed in the region of 1410–1540 cm^{-1}. From Fig. 1C, it is seen that commercial nimodipine consists mainly of mod I, with a small amount of mod II crystals, as evidenced by the absorption bands in the range 1410–1540 cm^{-1} (marked with a red circle), in agreement with the DSC and PXRD data.

Regarding the solid dispersions, microscopic observation under crossed polarizers showed the existence of strongly birefringent nimodipine microparticles. The physical form of nimodipine in the solid dispersions (choosing a representative formulation, F15 of Table 1) was further investigated by DSC, PXRD and FT-IR spectroscopy, and the corresponding results are illustrated in Fig. 2 in comparison with the data for the pure excipients used for their preparation. DSC thermograms of the solid dispersions, Fig. 2A, show a double endotherm at 58.6 and 61.3 °C that are attributed to the melting of PEG and polymorphs (standard and metastable folded chain form) [11]. The metastable form of PEG was not present after 3 months of storage. The thermograms lack any characteristic feature that can be used for the identification of nimodipine solid phase (crystalline mod I or II) present in the solid dispersions, in agreement with previous studies [33–35].

PXRD diffractograms of the effervescent floating formulations and the pure materials used for the preparation of dispersions (PEG 4000, PVP K30, HPMC K100M, sodium bicarbonate and citric acid), shown in Fig. 2B, indicate that PEG 4000, bicarbonate and citric acid exhibit intense reflections while HPMC K100 and PVP K30 only exhibit a halo that is characteristic of amorphous materials. PXRD diffractograms of the solid dispersions show additional reflections at 6.7°, 12.95° and 20.35° 2θ indicating the existence of nimodipine in the crystalline state, and specifically as mod I.

FT-IR spectra of the floating solid dispersions and pure excipients, illustrated in Fig. 2C, indicate that citric acid and HPMC K100 are the only materials that show absorbance in the region where the main differences between the amorphous and the crystal (mod I and mod II) nimodipine are located (at 3277 cm^{-1} for citric acid, and a broad peak at 3071–3640 cm^{-1} for HPMC K100). However, the characteristic peak of mod I at 3293 cm^{-1} is clearly seen in the floating solid dispersions' spectra, confirming the presence of nimodipine in the crystalline state. The presence of amorphous nimodipine in the solid dispersions can be excluded because of the existence of a strong sharp peak at 1693 cm^{-1}, characteristic of crystalline nimodipine and of the inalterability of the intensity and location of the peaks corresponding to the NH and C=O vibration of nimodipine mod I crystals after storage for 3 months at 25 °C – 60% RH and 40 °C – 75% RH.

The aforementioned findings, further supported by polarized light microscopy, indicate the high physical stability of the solid dispersions, which is a very important issue in the development of pharmaceutical formulations, and especially controlled release solid dispersions.

3.2. In vitro drug release

The drug content of the tablets subjected to dissolution testing varied between 98.3% and 102.5%, and their tensile strength was

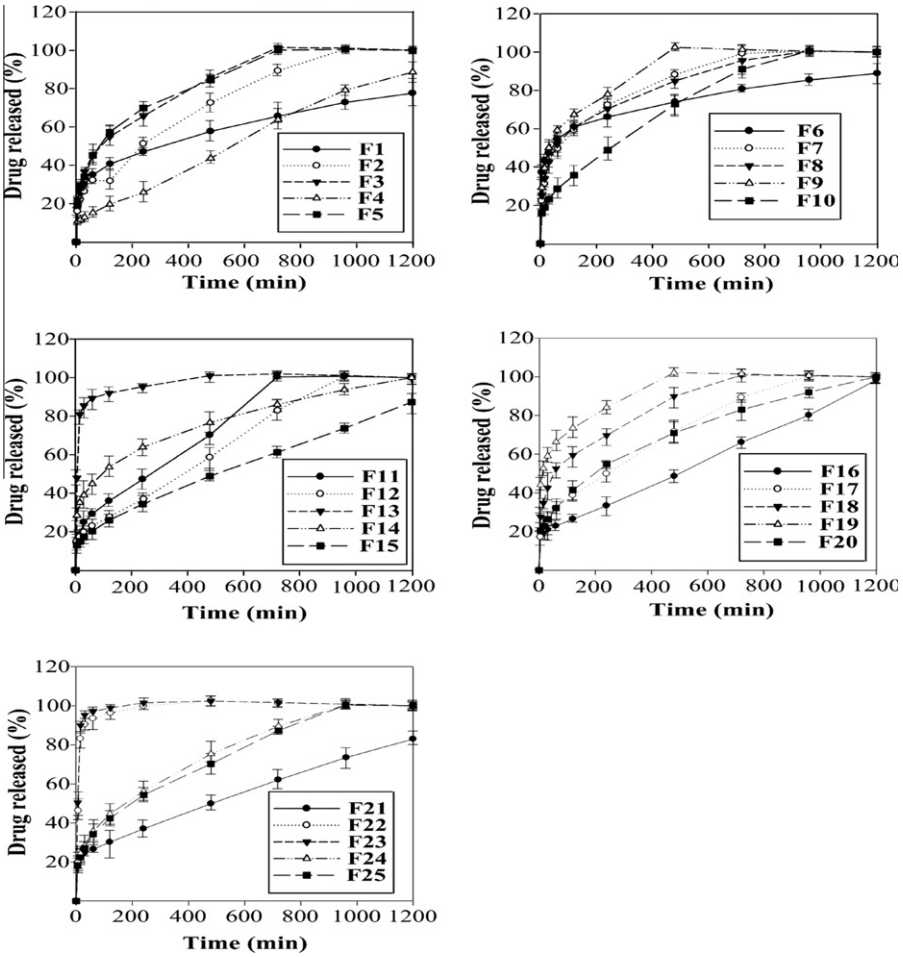

Fig. 3. Dissolution profiles of the floating tablet formulations proposed by the D-optimal experimental design.

between 51.4 N and 175.1 N. Due to the selection of a constant nimodipine content of 30 mg in all tablet formulations and the different proportions of excipients, tablet weights varied between 214 mg and 600 mg, leading to different initial surface area of the tablets. However, due to the extensive swelling and erosion of the polymer matrix, those initial differences are not expected to affect the dissolution ratio.

Dissolution profiles of the examined formulations are shown in Fig. 3, and corresponding values of the measured responses are listed in Table 4. From Fig. 3, it is seen that all formulations achieve prolongation of drug release except F13, F22 and F23 that contain high proportion of effervescent agents and show immediate release profiles (90% of the drug dissolved in less than 30 min). However, preliminary experiments showed that this effect of effervescent agents due to the generation of excess CO_2 was significantly reduced by the use of solid dispersions (19.6 ± 6% average reduction of percent drug release in 60 min, compared to physical mixtures). Concerning the release characteristics, increased amounts of HPMC contribute to a decrease in the release rate of nimodipine, contrary to the water-soluble PEG and PVP where increasing proportions lead to increasing release rates, in agreement with previous published studies concerning the role of these materials [36,37].

The mechanism of drug release was examined on the basis of the first-order, zero-order, Higuchi square root of time, Hixson–Crowell cube root and Korsmeyer–Peppas dissolution models summarized in Table 5 together with goodness of fit results for all examined formulations (mean coefficient of determination, R^2 ± standard deviation). Both the Korsmeyer–Peppas and zero-order kinetic models (after omitting the initial points corresponding to the burst effect) showed acceptable fit to the in vitro release data (R^2: 0.989 ± 0.010 and 0.980 ± 0.018, respectively), indicating that drug release was controlled by a combination of drug diffusion through the gel barrier formed by the hydrated polymer, and matrix erosion. This was confirmed by experimentally determined swelling and erosion parameters given in Table 6. Maximum water uptake (S_{max}) varied from 43.51% to 59.56%, while the dissolution medium uptake rate constant (a) of Eq. (3), and the apparent polymer erosion rate constant (k_2) of Eq. (4), varied from 3.46 $h^{-0.5}$ to 5.75 $h^{-0.5}$ and 0.03 × 10^{-3} h to 0.07 × 10^{-3} h. Increasing the proportions of HPMC, PEG and PVP contribute to an increase in maximum matrix swelling (S_{max}), while increasing the proportions of effervescent agents decreased S_{max}. The apparent matrix erosion rate (k_2) was increasing with the proportion of PEG and effervescent agents and decreasing with HPMC and PVP. The observed changes of the erosion rate can be attributed to the competing effects of the fast dissolving PEG and the effervescent agents that cause a disruption of the gel layer and of the highly viscous HPMC that swells and forms a gel layer that is further reinforced by the PVP.

Table 5
Release models and corresponding mean R^2 values for all formulations examined.

Model	Equation	Mean R^2 ± SD
First-order	$\ln(M) = kt$	0.851 ± 0.085
Zero-order	$M_0 - M = kt$	0.980 ± 0.018
Higuchi	$M_0 - M = kt^{1/2}$	0.790 ± 0.235
Hixson–Crowell	$M_0^{(1/3)} - M^{(1/3)} = kt$	0.716 ± 0.259
Korsmeyer–Peppas	$\log(M_0 - M) = \log(K) + n\log(t)$	0.989 ± 0.010

3.3. Floating behavior

The time needed for the initiation of flotation (floating lag time) was less than 3 min for all formulations (except those that showed immediate release profiles, F13, F22 and F23). Plots of continuous weight measurements as a function of time are shown in Fig. 4. The maximum floating strength, Fs, ranged from 0.31 g to 3.52 g while FLD varied from 1 h to 20 h, depending on the amount of CO_2 generated and the strength of the gel layer formed. Fs

Table 4
Experimental results collected according to the D-optimal mixture design for the selected response variables.

Formulation code	Measured responses			
	Y_{60min}[a] (%)	$t_{90\%}$[b] (h)	FLD[c] (h)	Fs[d] (g)
F1	13.9	24.0	20.0	2.82
F2	29.6	12.2	20.0	0.66
F3	45.5	9.1	8.3	2.29
F4	15.1	20.4	9.5	0.78
F5	45.1	9.5	11.1	2.59
F6	15.8	19.8	20.0	3.49
F7	39.4	9.0	11.0	1.85
F8	39.7	10.0	15.0	1.84
F9	59.2	4.9	6.3	2.24
F10	28.5	12.0	13.0	0.66
F11	27.9	10.4	9.1	0.65
F12	30.5	13.2	9.0	0.56
F13	89.3	1.3	3.0	3.40
F14	32.5	13.5	14.0	1.67
F15	15.7	21.0	9.4	1.20
F16	22.9	17.9	13.0	0.89
F17	32.0	12.5	9.4	0.69
F18	52.5	7.9	7.0	0.42
F19	66.2	4.6	7.2	0.41
F20	32.1	15.0	20.0	1.16
F21	14.7	21.7	20.0	0.31
F22	96.2	0.2	1.0	3.52
F23	96.9	0.2	1.0	3.51
F24	35.7	12.0	13.0	0.82
F25	33.0	12.0	12.5	0.83

SD: a = 1.01–3.28, b = 0.12–0.2, c = 0.09–1.29, d = 0.01–0.39.

Table 6
Parameters describing the swelling/erosion behavior of the examined formulations.

Code	Swelling			Erosion	
	S_{max}[a] (%)	a[b] ($h^{-0.5}$)	R^2	k_2[c] ($h^{-1} \times 10^3$)	R^2
F1	53.51	5.75	0.989	0.04	0.962
F2	55.27	3.85	0.999	0.05	0.973
F3	50.23	4.38	0.978	0.07	0.977
F4	54.46	4.35	0.906	0.05	0.988
F5	58.65	4.28	0.983	0.05	0.991
F6	52.61	4.13	0.961	0.04	0.981
F7	57.56	4.14	0.979	0.04	0.968
F8	58.56	4.15	0.981	0.04	0.953
F9	43.51	5.29	0.987	0.07	0.973
F10	54.46	4.68	0.952	0.07	0.998
F11	54.82	4.65	0.965	0.07	0.981
F12	59.56	4.57	0.975	0.04	0.994
F13*	–	–	–	–	–
F14	52.75	4.01	0.995	0.05	0.890
F15	57.56	4.35	0.930	0.04	0.977
F16	57.10	4.25	0.964	0.04	0.950
F17	56.61	4.34	0.962	0.06	0.938
F18	54.04	4.24	0.959	0.07	0.974
F19	55.26	4.43	0.962	0.07	0.969
F20	52.63	4.23	0.934	0.05	0.990
F21	58.62	4.46	0.966	0.03	0.985
F22[d]	–	–	–	–	–
F23[d]	–	–	–	–	–
F24	54.10	3.66	0.999	0.08	0.993
F25	55.78	3.46	0.998	0.08	0.991

[a] SD = 1.18–4.5.
[b] SD = 0.05–0.21.
[c] SD = 0.02–2.0.
[d] F13, F22 and F23 showed immediate release profile.

increased as the proportion of effervescent agents and HPMC increased while FLD decreased as the proportion of HPMC and effervescent agents decreased (weaker gel layer and smaller amount of CO_2 generated).

3.4. Optimization of drug formulation

3.4.1. Artificial neural networks

The optimum network consisted of one hidden layer with 6 units, Fig. 5A, while the optimum number of training cycles was found to be 4000. Results of input variable importance, Table 7, indicate that the proportion of effervescent agent (EFF) is the most influential variable closely followed by HPMC, while PEG and PVP are of a relatively minor importance. Moreover, the pruned (simplified) network by the MBP algorithm, shown in Fig. 5B, contained only 2 units in the hidden layer, while only three inputs (HPMC, EFF and nimodipine proportion) were preserved, in agreement with the described variable importance results.

3.4.2. Genetic programming

The application of symbolic regression by GP resulted in the following equations for the correlation of the formulation factors with the selected responses:

$$Y_{60\text{min}} = 0.29^{\wedge}(\sin((\tan(X_1) - \log(X_5)))^{\wedge}(((X_4 - X_3)/(X_3 * X_5)) + (\tan(X_4)/(X_4/X_1)))) \quad (6)$$

$$t_{90\%} = ((\cos(\cos((X_2 * X_5))) * (\tan((X_3^{\wedge}X_3))/\exp((X_1 + X_5))))^{\wedge}(\sin(\tan(X_4/X_4))/\exp(\cos(\tan(X_4))))) \quad (7)$$

$$\text{FLD} = (\cos((\exp(X_1)^{\wedge}(X_4 - X_3)))^{\wedge}\sin(\exp((X_5 - X_4)))) \quad (8)$$

$$\text{Fs} = (((X_4^{\wedge}2)^{\wedge}(X_1 + X_3))^{\wedge}((X_4 + X_5)^{\wedge}\exp(X_2))) \quad (9)$$

All GP-derived equations (Eq. (6)–(9)) highlight the nonlinear nature between the dependant and independent variables. In agreement to previous sensitivity and saliency results, formulation factor X_2 (PVP) was not included in Eq. (6) and (8), indicating its insignificant effect at least on the burst effect ($Y_{60\text{min}}$) and floating strength (Fs). However, the factor was retained in the design, since it seems to exert a significant effect on the rest of the examined responses.

3.4.3. Validation of ANN and GP

The predictive ability of the ANN and GP models was evaluated on an external validation set (Table 3), on the basis of RMSEp values listed in Table 8. It is seen that both ANN and symbolic

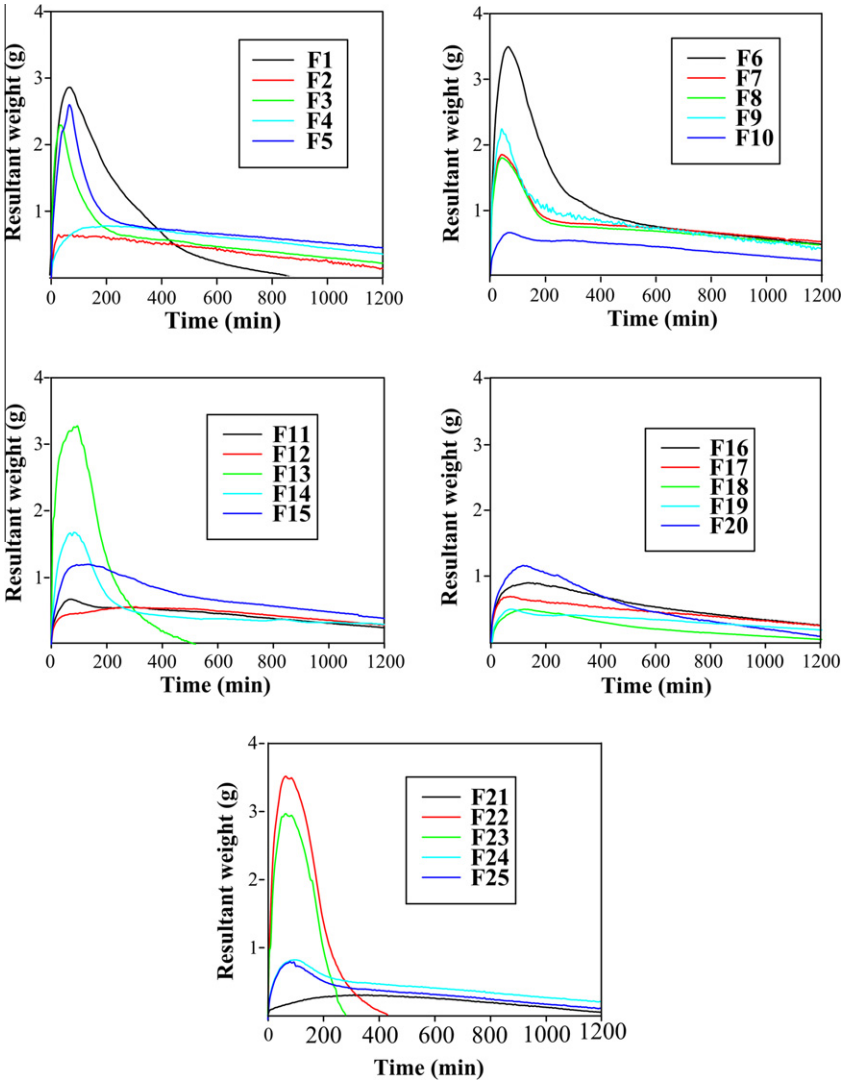

Fig. 4. Weight versus time profiles for the evaluation of tablet floating behavior.

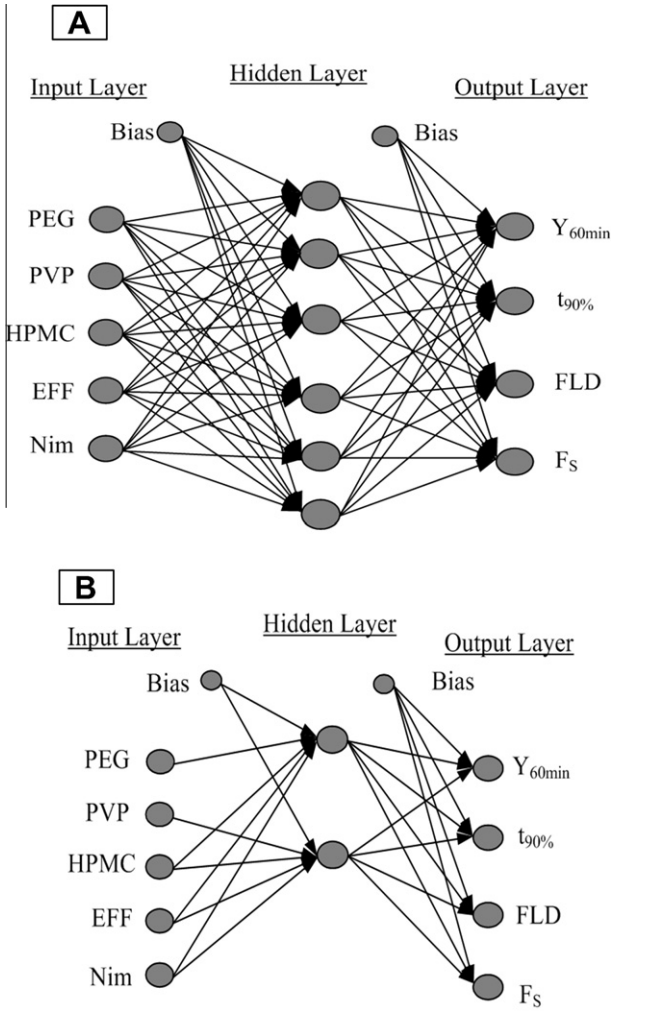

Fig. 5. Optimum neural network architecture using PEG, PVP, HPMC, effervescent agents (EFF) and nimodipine (NIM) as independent factors and $Y_{60\ min}$, $t_{90\%}$, FLD and Fs as responses, before (A) and after pruning (B).

Table 7
Causal (sensitivity) and predictive importance (saliency) of the examined input variables.

Input variable	Sensitivity	Saliency
PEG	1.98	0.18
PVP	2.66	0.60
HPMC	5.62	2.76
EFF	5.84	3.14
NIM	3.79	2.62

Table 8
Predictive ability (RMSEp) based on the selected external validation set (Table 3) for the generated ANN and GP models.

Responses	RMSEp		
	ANN		GP
	StBack	MBP	
Y_{60min}	0.0193	0.0186	0.0184
$t_{90\%}$	0.0227	0.0354	0.0265
FLD	0.0438	0.0782	0.0589
F_S	0.0590	0.0613	0.0588

regression via GP have equally good prediction performance, probably due to the high nonlinear nature of both ANN and GP models. Moreover, the close approximation in RMSEp for the original and pruned ANN indicates that a good level of predictive performance can be preserved while simplifying network's structure.

3.4.4. Multi-objective optimization

Since GP produces equations of substantially lower complexity than the ANN models, it was selected as the best-fitting model, according to the parsimony principle in statistics. The minimization of the standardized Euclidian distance (Eq. (5)) between the predicted and the optimum values of each response, resulted in a tablet consisting of 9% PEG, 30% PVP, 36% HPMC, 11% EFF and 14% nimodipine. From the dissolution and the floating kinetics profile of the optimum floating formulation, Fig. 6, it is seen that the selected responses were within the desirable target levels (Y_{60min} = 15.1%, $t_{90\%}$ = 12.1 h, Fs = 0.89 g and was over 9.5 h). The Fs value of the optimum formulation was the maximum attainable without compromising the values of the remaining optimized responses (controlled release profile and floating duration).

Furthermore, swelling and erosion of the optimum formulation, evaluated graphically (Fig. 7), suggest that it undergoes swelling followed by extensive erosion, attaining maximum water uptake (S_{max} = 44.57%) at 4 h that is compensated by the weight loss due

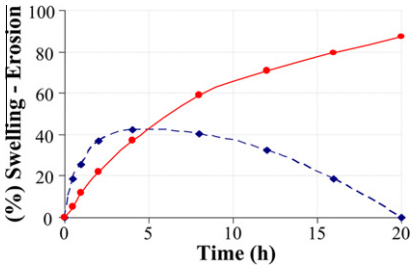

Fig. 7. Swelling (dashed line) and erosion (solid line) profiles of the optimum formulation proposed by GP.

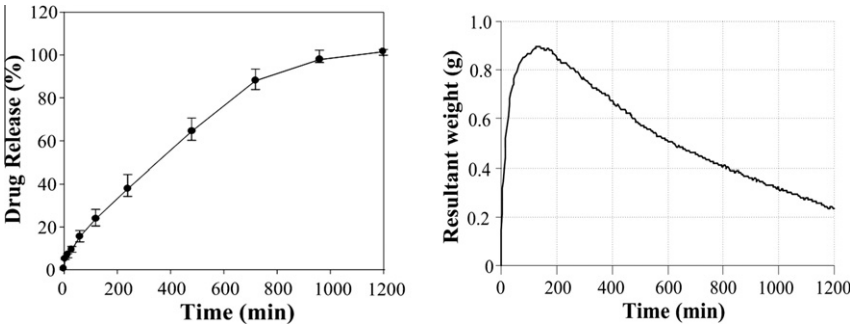

Fig. 6. Drug release and floating kinetics profile of the optimum controlled released formulation proposed by GP.

to matrix erosion after 5 h. Generally, it can be concluded that matrix erosion predominated in the API's release.

4. Conclusion

The present study demonstrates the development of a nimodipine effervescent floating controlled release tablet formulation using solid dispersions. A microcrystalline dispersion of nimodipine mod I was formed in the PEG matrix, while the combination of experimental design and modern machine learning algorithms such as ANNs and GP showed increased prediction efficiency during the optimization procedure. Simultaneous swelling and erosion were identified as the main mechanisms of API release from the floating tablet formulations.

Acknowledgments

The authors wish to thank Dr. Jason H. Moore, professor of Genetics and Community & Family Medicine in Dartmouth Medical School and Mr. Peter Andrews programmer in Computational Genetics Lab Dartmouth Medical Centre for their help with the GP software tool (SyMod).

References

[1] A. Grunenberg, B. Keil, J.O. Henck, Polymorphism in binary mixtures, as exemplified by nimodipine, Int. J. Pharm. 118 (1995) 11–21.
[2] M.S. Langley, E.M. Sorkin, Nimodipine a review of its pharmacodynamic and pharmacokinetic properties, and therapeutic potential in cerebrovascular disease, Drugs 37 (1989) 669–699.
[3] W. Wu, Q. Zhou, H.B. Zhang, G.D. Ma, C.D. Fu, Studies on nimodipine sustained-release tablet capable of floating on gastric fluid with prolonged gastric resident time, Acta Pharm. Sinica 32 (1997) 786–790.
[4] S.J. Wie, J.P. Liu, R. Lu, W.J. Zheng, Release kinetics and in vitro-in vivo correlation of nimodipine sustained-release soft gelatin capsule, Chin. Pharm. J. 42 (2007) 852–856.
[5] P. Barmpalexis, F.I. Kanaze, K. Kachrimanis, E. Georgarakis, Artificial neural networks in the optimization of a nimodipine controlled release tablet formulation, Eur. J. Pharm. Biopharm. 74 (2010) 316–323.
[6] M. Ichikawa, S. Watanabe, Y. Miyake, A new multiple unit oral floating dosage system. I: preparation and in vitro evaluation of floating and sustained-release kinetics, J. Pharm. Sci. 80 (1991) 1062–1066.
[7] N. Ozdemir, S. Ordu, Y. Ozkan, Studies of floating dosage forms of furosemide: in vitro and in vivo evaluation of bilayer tablet formulation, Drug Dev. Ind. Pharm. 26 (2000) 857–866.
[8] M.C. Gohel, G. Manhapra-Sumitra, Modulation of active pharmaceutical material release from a novel 'tablet in capsule system' containing an effervescent blend, J. Control. Release 79 (2002) 157–164.
[9] S. Arora, J. Ali, A. Ahuja, R.K. Khar, S. Baboota, Floating drug delivery systems: a review, AAPS PharmSciTech. 6 (2005) E372–E390.
[10] T. Ozeki, H. Yuasa, Y. Kanaya, Controlled release from solid dispersion composed of poly(ethylene oxide)–Carbopol® interpolymer complex with various cross-linking degrees of Carbopol®, J. Control. Release 63 (2000) 287–295.
[11] D.Q.M. Graig, The mechanism of drug release from solid dispersions in water-soluble polymers, Int. J. Pharm. 231 (2002) 131–144.
[12] FDA Guidance for Industry, PAT – A Framework for Innovative Pharmaceutical Development, Manufacturing, and Quality Assurance, 2004.
[13] FDA Guidance for Industry, Quality Systems Approach to Pharmaceutical CGMP Regulations, 2006.
[14] International Conference on Harmonization (ICH) Proceedings, Q8(R2): Pharmaceutical Development, US FDA Federal Register, 2009.
[15] F. Castillo, K. Marshall, J. Green, A. Kordon, A methodology for combing symbolic regression and design of experiments to improve empirical model building, in: G. Bittencourt, G.L. Ramalho (Eds.), Advances in Artificial Intelligence, Springer, Berlin Heidelberg, 2002, pp. 345–354.
[16] K. Takayama, M. Fujikawa, Y. Obata, M. Morishita, Neural network based optimization of drug formulation, Adv. Drug Deliv. Rev. 55 (2003) 1217–1231.
[17] D.Q. Do, R.C. Rowe, P. York, Modelling drug dissolution from controlled release products using genetic programming, Int. J. Pharm. 351 (2008) 194–200.
[18] J. Takahara, K. Takayama, T. Nagai, Multi-objective simultaneous optimization technique based on an artificial neural network in sustained release formulation, J. Control. Release 49 (1997) 11–20.
[19] K. Takayama, A. Morva, M. Fujikawa, Y. Hattori, Y. Obata, T. Nagai, Formula optimization of theophylline controlled-release tablet based on artificial neural networks, J. Control. Release 68 (2000) 175–186.
[20] European Pharmacopoeia, fifth ed., Monographs, Council of Europe, cop. Strasbourg, 2008, pp. 1981–1982.
[21] P. Barmpalexis, F.I. Kanaze, E. Georgarakis, Developing and optimizing a validated isocratic reversed-phase high-performance liquid chromatography separation of nimodipine and impurities in tablets using experimental design methodology, J. Pharm. Biomed. Anal. 49 (2009) 1192–1202.
[22] J. Timmermans, A.J. Moës, How well do floating dosage forms float?, Int J. Pharm. 62 (1990) 207–216.
[23] H.Y. Karasulu, F. Taneri, E. Sanal, T. Guneri, G. Ertan, Sustained release bioadhesive effervescent ketoconazole mictocapsules tabletted for vaginal delivery, J. Microencapsul. 19 (2002) 357–362.
[24] L. Wang, X. Tang, A novel ketoconazole bioadhesive effervescent tablet for vaginal delivery: design, in vitro and in vivo evaluation, Int. J. Pharm. 350 (2008) 181–187.
[25] N. Kavanagh, O.I. Corrigan, Swelling and erosion properties of hydroxypropylmethylcellulose (Hypromellose) matrices-influence of agitation rate and dissolution medium composition, Int. J. Pharm. 279 (2004) 141–152.
[26] K. Tahara, K. Yamamoto, T. Nishihata, Overall mechanism behind matrix sustained release (SR) tablets prepared with hydroxypropyl methylcellulose, J. Control. Release 35 (1995) 59–66.
[27] S.F. Ahrabi, G. Madsen, K. Dyrstad, S.A. Sande, C. Graffner, Development of pectin matrix tablets for colonic delivery of model drug ropivacaine, Eur. J. Pharm. Sci. 10 (2000) 43–52.
[28] K. Kachrimanis, V. Karamyan, S. Malamataris, Artificial neural networks (ANNs) and modeling of powder flow, Int. J. Pharm. 250 (2003) 13–23.
[29] J.R. Koza, Genetic programming as means for programming computers by natural selection, Stat. Comput. 4 (1994) 87–112.
[30] E. Spinoza, A. Pozo, Controlling the population size in genetic programming, in: E. Cantu-Paz, J.A. Foster, K. Deb, L.D. Davis, R. Roy, U.M. O'Reilly, H.G. Beyer, R. Standish, G. Kendall, S. Wilson, M. Harman, J. Wegener, D. Dasgupta, M.A. Potter, A.C. Schultz, K.A. Dowsland, N. Jonoska, J. Miller (Eds.), Genetic and Evolutionary Computation-GECCO, Springer, Berlin, Heidelberg, 2003, pp. 1975–1985.
[31] S. Agatonovic-Kustrin, R. Beresford, Basic concepts of artificial neural network (ANN) modeling and its application in pharmaceutical research, J. Pharm. Biomed. Anal. 22 (2000) 717–727.
[32] X.C. Tang, M.J. Pikal, L.S. Taylor, A spectroscopic investigation of hydrogen bond patterns in crystalline and amorphous phases in dihydropyridine calcium channel blockers, Pharm. Res. 19 (4) (2002) 477–483.
[33] N.A. Urbanetz, B.C. Lippold, Solid dispersions of nimodipine and polyethylene glycol 2000: dissolution properties and physico-chemical characterization, Eur. J. Pharm. Biopharm. 59 (2005) 107–118.
[34] M.M. Smikalla, N.A. Urbanetz, The influence of povidone K17 on the storage stability of solid dispersions of nimodipine and polyethylene glycol, Eur. J. Pharm. Biopharm. 66 (2007) 106–112.
[35] G.Z. Papageorgiou, D. Bikiaris, E. Karavas, S. Politis, A. Docoslis, Y. Park, A. Stergiou, E. Georgarakis, Effect of physical state and particle size distribution on dissolution enhancement of Nimodipine/PEG solid dispersions prepared by melt mixing and solvent evaporation, AAPS J. 8 (4) (2006) E623–E631.
[36] M. Vlachou, N. Hani, M. Efentakis, P.A. Tarantili, A.G. Andreopoulos, Polymers for use in controlled release systems: the effect of surfactants on their swelling properties, J. Biomater. Appl. 15 (2000) 65–77.
[37] Y.B. Huang, Y.H. Tsai, W.C. Yang, J.S. Chang, P.C. Wu, K. Takayama, Once-daily propranolol extended-release tablet dosage form: formulation design and in vitro/in vivo investigation, Eur. J. Pharm. Biopharm. 58 (2004) 607–614.